Systems for Orthogonal Self-Assembly of Electroactive Monolayers on Au and ITO: An Approach to Molecular Electronics

Timothy J. Gardner, C. Daniel Frisbie, and Mark S. Wrighton*

Contribution from the Department of Chemistry, Massachusetts Institute of Technology, Cambridge, Massachusetts 02139

Received November 7, 1994®

Abstract: Simultaneous exposure of Au and In_2O_3/SnO_2 (ITO) electrodes to an equimolar solution of a thiol and a carboxylic acid or a thiol and phosphonic acid results in the selective attachment of the thiol to the Au electrode and the carboxylic or phosphonic acid to the ITO electrode. This selective surface-attachment chemistry is termed "orthogonal self-assembly" (OSA) and can be used to direct the spontaneous assembly of molecular reagents onto Au and ITO microstructures. The selectivity of the thiols for Au and the carboxylic or phosphonic acids for ITO is determined by a combination of cyclic voltammetry experiments using ferrocene-tagged molecules, scanning Auger microscopy, and imaging secondary ion mass spectrometry (SIMS) to map the distribution of thiols, carboxylic acids, and phosphonic acids on derivatized Au and ITO microstructures. Simultaneous exposure of Au and ITO electrodes for 30 min to an equimolar solution of 11-mercaptoundecanoylferrocene (**I**) and 12-ferrocenyldodecanoic acid (**III**) results in a coverage ratio I:**III** of approximately 100:1 on Au and 1:45 on ITO, as determined by cyclic voltammetry. A 30-min exposure of Au and ITO electrodes to an equimolar solution of **I** and 6-ferrocenylhexylphosphonic acid (**V**) yields a coverage ratio of **I**:**V** of 30:1 on Au and better than 1:100 on ITO. The coverages of **I**, **III**, and **V** on the Au and ITO electrodes can be determined using cyclic voltammetry by virtue of the difference in redox potential between the acylferrocene center in **I** and the alkylferrocene centers in **III** and **V**. Typical converages of **I** on Au (4×10^{-10} mol/cm^2) and **III** and **V** on ITO (6×10^{-10} and 3×10^{-10} mol/cm^2, respectively) after 30 min of derivatization correspond to approximately a monolayer of redox-active molecules in each case. Long derivatization times (12–15 h) result in small or insignificant changes in the coverage ratios of these reagents on both Au and ITO electrodes, demonstrating that the OSA is essentially complete within 30 min. Surface analysis by X-ray photoelectron spectroscopy, scanning Auger microscopy, and imaging SIMS of Au and ITO microstructures and Si_3N_4 surfaces exposed to equimolar solutions of **I** and perfluorodecanoic acid (**IV**), or 12,12,12-trifluorododecanethiol (**II**) and **V**, reveal the selective assembly of these reagents on the Au and ITO microstructures and their absence on the insulating Si_3N_4 substrate. The orthogonal self-assembly process described here provides a promising method by which individual molecules could be spontaneously oriented and connected between closely-spaced, externally-addressable electrodes.

Introduction

We wish to report two systems which can be used to simultaneously assemble two unique molecular reagents, L_1 and L_2, as independent monolayers on two different substrates, Au and indium tin oxide (ITO), as shown in Scheme 1. We call the process depicted in Scheme 1 "orthogonal self-assembly"[1,2] since exposure of the two different materials, Au and ITO, to a single solution containing both L_1 and L_2 results in the selective attachment of L_1 molecules to Au and L_2 molecules to ITO. In the work reported here, L_1 molecules are functionalized thiols **I** and **II**, and L_2 molecules are functionalized carboxylic acids **III** and **IV**,[3] or the functionalized phosphonic acid **V**.[4]

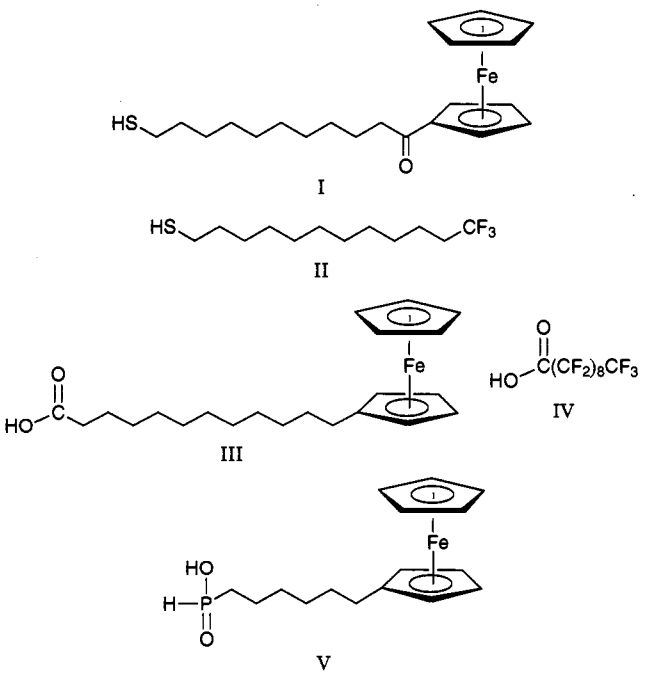

* Address correspondence to this author.

® Abstract published in *Advance ACS Abstracts*, April 15, 1995.

(1) (a) Laibinis, P. E.; Hickman, J. J.; Wrighton, M. S.; Whitesides, G. M. *Science* **1989**, *245*, 845. (b) Hickman, J. J.; Laibinis, P. E.; Auerbach, D. I.; Zou, C.; Gardner, T. J.; Whitesides, G. M.; Wrighton, M. S. *Langmuir* **1992**, *8*, 357.

(2) (a) Nuzzo, R. G.; Allara, D. L. *J. Am. Chem. Soc.* **1983**, *105*, 4481. (b) Nuzzo, R. G.; Zegarski, B. R.; Dubois, L. H. *J. Am. Chem. Soc.* **1987**, *109*, 733. (c) Swalen, J. D.; Allara, D. L.; Andrade, J. D.; Chandross, E. A.; Garoff, S.; Israelachvili, J.; McCarthy, T. J.; Murray, R. W.; Pease, R. F.; Rabolt, J. F.; Wynne, K. J.; Yu, H. *Langmuir* **1987**, *3*, 932 and references therein. (d) Strong, L.; Whitesides, G. M. *Langmuir* **1988**, *4*, 546. (e) Wasserman, S. R.; Tao, Y.-T.; Whitesides, G. M. *Langmuir* **1989**, *5*, 1074. (f) Bain, C. D.; Whitesides, G. M. *J. Am. Chem. Soc.* **1989**, *111*, 7164. (g) Whitesides, G. M.; Laibinis, P. E. *Langmuir* **1990**, *6*, 87. (h) Chidsey, C. E. D.; Bertozzi, C. R.; Putvinski, T. M.; Mujsce, A. M. *J. Am. Chem. Soc.* **1990**, *112*, 4301. (i) Ulman, A. *An Introduction to Ultrathin Organic Films From Langmuir-Blodgett to Self-Assembly*; Academic Press: Boston, MA, 1991.

0002-7863/95/1517-6927$09.00/0

Scheme 1. Orthogonal Self-Assembly of Molecules L_1 and L_2 onto Electrodes Made of Two Different Materials

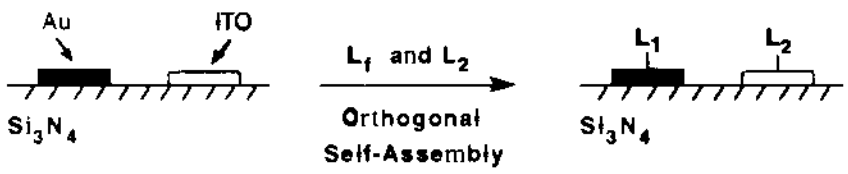

We have previously shown orthogonal self-assembly (OSA) for two other systems: (1) Au and Al_2O_3 microstructures exposed to a solution of substituted thiols and carboxylic acids,[1a] and (2) plasma-treated Au and Pt surfaces exposed to a solution of substituted disulfides and isonitriles.[1b] As will be clarified below, the first system suffers from the disadvantage that one of the materials, Al_2O_3, is not electrically conductive. The second system unfortunately involves exposure of Au and Pt surfaces to non-equimolar solutions of the disulfide and isonitrile. The significance of our new results presented here is that we have found two systems by which the OSA process in Scheme 1 can be achieved from an *equimolar* solution of reagents L_1 and L_2 using two electrically conductive materials, Au and ITO, as substrates.

The motivation for this work comes from previous efforts to fabricate molecule-based sensors[5] and microelectrochemical transistors.[6] Microelectrochemical transistors are devices which exploit the properties of molecular materials to achieve "switching" or amplification of electrical or chemical signals. Aside from their possible application as chemical sensors, microelectrochemical transistors have proved useful in studying the conductivities of molecular materials over small domains (<200 nm).[6b,d,e] A major goal in our laboratory has been to reduce the number of molecules probed or switched in these conductivity measurements by reducing the overall dimensions of the device. A truly molecular-scale device in which the electrical characteristics of individual molecules are probed would be of fundamental scientific value, if it could be constructed. We, and others, have proposed approaches to the making of "molecular wires" which could connect a pair of very closely spaced (<50 nm) electrodes,[7a] and a recent article has examined the progress in this area of research.[7b] Balazs *et al.* have theorized about how molecules might interact with electrode structures,[8] and Hopfield *et al.* have proposed memory devices based on molecular wires.[9]

If molecular-scale devices are to be realized, there must be practical methods to make external connections to the constituent molecules. We believe that OSA provides a promising method

Scheme 2

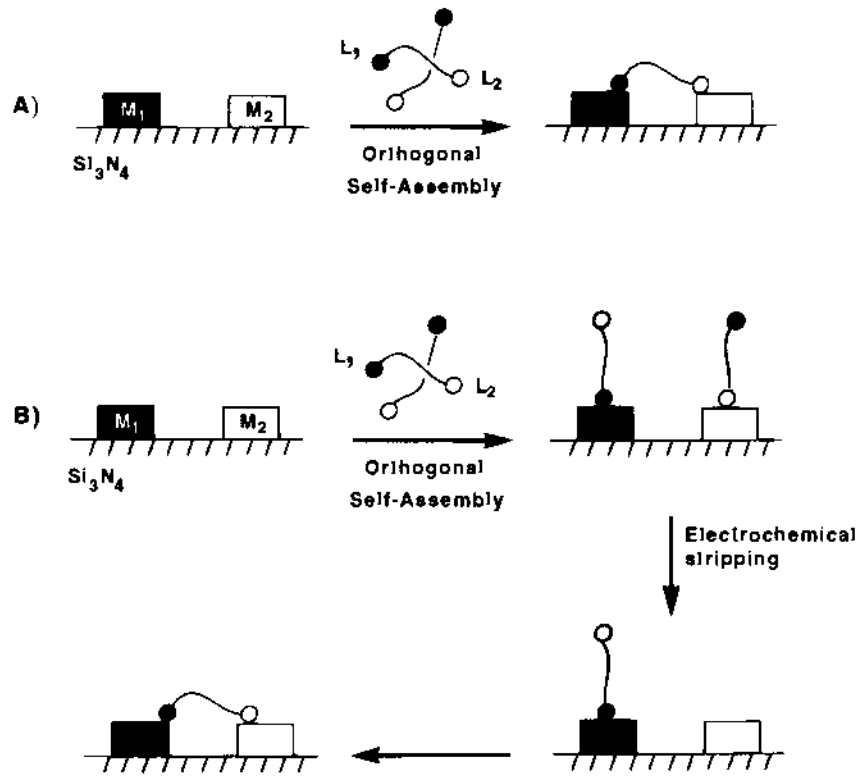

by which both attachment to electrical contacts and *orientation* of a macromolecule can be achieved. Scheme 2 illustrates two possible approaches for assembling a macromolecule between two electrodes composed of different materials, M_1 and M_2, using orthogonal self-assembly. In approach A, immersion of closely-spaced M_1 and M_2 electrodes into a solution of a bifunctional macromolecule results in spontaneous orientation and attachment of the molecule between the electrodes. This approach might be favored, for instance, if the rate of L_1 binding to M_1 is substantially greater than the rate of L_2 binding to M_2. In that case, macromolecules would bind to M_1 via L_1 and then the dangling L_2 groups at the other end of the molecule would be free to bind to the essentially naked M_2 electrode. Approach B accounts for the possibility that electrodes M_1 and M_2 are each initially completely covered by macromolecules upon immersion into the derivatization solution. Subsequent electrochemical stripping of molecules from the M_2 electrode[10] would allow the dangling L_2 ligands on the macromolecule attached to M_1 to bind to M_2, as shown in the scheme. Both approaches A and B result in the same final structure with the macromolecule oriented and connected on either end by electrodes M_1 and M_2. The key to achieving the oriented connection is that the surface-attachment ligands, L_1 and L_2, must be strongly selective for the two different electrode materials.

The attachment strategies outlined in Scheme 2 are the motivation behind our search for OSA systems which employ equimolar concentrations of reagents L_1 and L_2. We note that because OSA is a molecular self-assembly method, creating structures like that shown in Scheme 2 could be done at the size limits imposed by present or future nanofabrication technology. Importantly, regardless of the eventual utility or practicality of molecule-based devices, OSA as a means of surface modification should prove useful to orient molecules between dissimilar metals to achieve electronic or non-linear optical effects, or to facilitate basic studies of electron transfer and conduction in individual molecules of interest.

Experimental Section

Reagents. Au (99.999%) for electron beam deposition was obtained from Materials Research Corp. (Orangeburg, NY). ITO (91% In_2O_3 and 9% SnO_2 in chunk form) was obtained from Cerac (Milwaukee,

(3) Laibinis, P. Harvard University, personal communication of unpublished XPS data taken while a member of the George Whitesides group, indicated that *n*-alkyl carboxylic acids chemisorbed onto ITO preferentially over *n*-alkyl thiols present in the same derivatizing solution.

(4) (a) Yang, H. C.; Aoki, K.; Hong, H.-C.; Sackett, D. D.; Arendt, M. F.; Yau, S.-L.; Bell, C. M.; Mallouk, T. E. *J. Am. Chem. Soc.* **1993**, *115*, 11855. (b) Hong, H.-G.; Mallouk, T. E. *Langmuir* **1991**, *7*, 2362.

(5) (a) Rubinstein, I.; Steinberg, S.; Tor, Y.; Shanzer, A.; Sagiv, J. *Nature* **1988**, *332*, 426. (b) Mirkin, C. A.; Wrighton, M. S. *J. Am. Chem. Soc.* **1990**, *112*, 8596. (c) Hickman, J. J.; Ofer, D.; Laibinis, P. E.; Whitesides, G. M.; Wrighton, M. S. *Science* **1991**, *252*, 688.

(6) (a) Kittlesen, G. P.; White, H. S.; Wrighton, M. S. *J. Am. Chem. Soc.* **1984**, *106*, 7389. (b) Paul, E. W.; Ricco, A. J.; Wrighton, M. S. *J. Phys. Chem.* **1985**, *89*, 1441. (c) Kittlesen, G. P.; Wrighton, M. S. *J. Mol. Electron.* **1986**, *2*, 23. (d) Jones, E. T. T.; Chyan, O. M.; Wrighton, M. S. *J. Am. Chem. Soc.* **1987**, *109*, 5526. (e) Ofer, D.; Crooks, R. M.; Wrighton, M. S. *J. Am. Chem. Soc.* **1990**, *112*, 7869. (f) Talham, D. R.; Crooks, R. M.; Canimarata, V.; Leventis, N.; Schloh, M. O.; Wrighton, M. S. Lower-Dimensional Systems and Molecular Electronics; Metzger, R. M., Day, P., Papavassiliou, G., Eds.; NATO ASI Series; Plenum Press: New York, 1991; pp 657–664. (g) McCoy, C. H.; Wrighton, M. S. *Chem. Mater.* **1993**, *5*, 914.

(7) (a) Dagani, R. *Chem. Eng. News* **1991**, *69*(21), 24. (b) Dagani, R. *Chem. Eng. News* **1993**, *71*(12), 20.

(8) Balazs, A.; Huang, K.; Lantman, C. *Macromolecules* **1990**, *23*, 4641.

(9) Hopfield, J.; Onuchic, J.; Beratan, D. *J. Phys. Chem.* **1989**, *93*, 6350.

(10) Walczak, M. M.; Popenoe, D. D.; Deinhammer, R. S.; Lamp, B. D.; Chung, C.; Porter, M. D. *Langmuir* **1991**, *7*, 2687.

WI). All solvents were spectroscopic grade. Electrolytes were reagent grade or better and were recrystallized. The synthesis of 11-mercaptoundecanoylferrocene (**I**)[11] has been described elsewhere. 12,12,12-trifluorododecanethiol, **II**, was a gift from Hans Biebuyck of Harvard University. Perfluorodecanoic acid, **IV**, is available commercially from Aldrich (Milwaukee, WI), and was used as received.

Synthesis. (a) 11-Bromoundecanoyl Chloride. 11-Bromoundecanoic acid (13.1 g, 50 mmol; Aldrich) was dissolved in CH_2Cl_2 under N_2. $SOCl_2$ (7.3 mL, 100 mmol) was added to this solution via syringe, and the mixture was refluxed for 4 h. Distillation under vacuum produced 11-bromoundecanoyl chloride (147 °C at 2 mmHg) which was stored at 5 °C.

(b) 11-Bromoundecanoylferrocene. Ferrocene (3.2 g, 17 mmol) was placed in a 200-mL round-bottomed flask and dissolved in CH_2Cl_2 with stirring. A CH_2Cl_2 solution of 4.9 g (17 mmol) of 11-bromoundecanoyl chloride and 2.4 g (18 mmol) of $AlCl_3$ was added slowly from a graduated cylinder. This solution was stirred at room temperature under N_2 for 12 h. The reaction mixture was then poured into a separatory funnel and washed with saturated aqueous NaOH. The organic phase was removed *in vacuo* leaving a brown solid. Column chromatography on silica gel (EM Science) with hexane separated the unreacted ferrocene and 1,1′-bis(11-bromoundecanoyl)-ferrocene from the desired product (3 g, 7 mmol). ^{1}H NMR (Bruker 250 MHz) (C_6D_6) δ 4.68 (t, 2H), 4.08 (t, 2H), 3.94 (s, 5H), 2.97 (t, 2H), 2.55 (t, 2H), 1.83 (m, 2H), 1.55 (m, 2H), 1.4−1.0 (m, 12H).

(c) 11-Bromoundecylferrocene. 11-Bromoundecylferrocene was obtained by Clemmensen reduction of 11-bromoundecanoylferrocene. Hg/Zn amalgam was prepared by mixing 8.6 g (132 mmol) of Zn with 0.86 g (3 mmol) of $HgCl_2$ in 10 mL of H_2O with 0.6 mL of concentrated HCl, stirring for 15 min, and filtering. 11-Bromoundecanoylferrocene (3 g, 7 mmol) was added to a round-bottomed flask containing 50 mL of toluene, 13 mL of concentrated HCl, and 6 mL of H_2O along with the Hg/Zn. The solution was refluxed under N_2 with vigorous stirring for 2 days. Product was isolated by washing the reaction mixture with aqueous $NaHCO_3$, separating and evaporating the organic phase, followed by chromatography with 1:1 hexane:ether on silica gel. ^{1}H NMR (Bruker 250 MHz) (C_6D_6) δ 4.05 (s 5H), 4.02 (t, 2H), 3.99 (t, 2H), 2.95 (t, 2H), 2.26 (t, 2H), 1.55 (m, 4H), 1.4−1.0 (m, 14H).

(d) 11-Cyanoundecylferrocene. 11-Bromoundecylferrocene (1.34 g, 3.2 mmol) was dissolved in 20 mL of acetonitrile under N_2. 18-Crown-6 (0.08 g, 0.3 mmol; Aldrich) and 0.42 g (6.4 mmol) of KCN were added to this solution. The mixture was refluxed for 10 h. The acetonitrile was removed *in vacuo*, and the remaining residue was chromatographed on silica gel with hexane:diethyl ether (5:1). 11-Cyanoundecylferrocene (1.05 g, 2.9 mmol) was recovered. ^{1}H NMR (Bruker 250 MHz) (C_6D_6) δ 4.05 (s, 5H), 4.02 (t, 2H), 3.99 (t, 2H), 2.33 (t, 4H), 1.54 (m, 4H), 1.4−0.8 (m, 14H).

(e) 12-Ferrocenyldodecanoic acid (III). 11-Cyanoundecylferrocene (1.05 g, 2.9 mmol) was dissolved in 20 mL of C_2H_5OH:H_2O (1:1). KOH (0.56 g, 10 mmol) in H_2O was added, and the reaction was stirred for 3 h. The reaction mixture was acidified to pH 2 with HCl and extracted with CH_2Cl_2. The organic phase was evaporated and the residue chromatographed on silica gel with CH_2Cl_2:hexane (2:1). 12-Ferrocenyldodecanoic acid (0.9 g, 2.3 mmol) was recovered, as identified by ^{1}H NMR and mass spectrometry ($M^+ = 384$). ^{1}H NMR (Bruker 250 MHz) (C_6D_6) δ 4.05 (s, 5H), 4.02 (t, 2H), 3.99 (t, 2H), 2.31 (t, 2H), 2.08 (t, 2H), 1.52 (m, 4H), 1.4−1.1 (m, 14H).

(f) 6-Ferrocenylhexylphosphonic Acid (V). **V** was obtained by hydrolysis of diethyl 6-ferrocenylhexylphosphonate, the synthesis of which has been reported.[12] The hydrolysis was performed analogous to the method of Rabinowitz:[13] Diethyl 6-ferrocenylhexylphosphonate (0.5 g, 1.2 mmol) was dissolved in dry CH_2Cl_2 under N_2. Trimethylbromosilane (0.5 mL, 3 mmol; Aldrich) was added to the solution via syringe, and the solution was stirred at room temperature. After 12 h, the solvent and excess trimethylbromosilane were removed *in vacuo* leaving a yellow solid which was shown to be the silyl ester by ^{1}H NMR. The silyl ester was dissolved in 200 mL of methanol and the solution was stirred for 5 min, followed by removal of the methanol *in vacuo*. This hydrolysis procedure was repeated three times yielding a yellow solid which was identified as 6-ferrocenylhexylphosphonic acid ^{1}H NMR (Bruker AC250) ($(CD)_3CO$) δ 3.95 (s, 5H), 3.93 (t, 2H), 3.90 (t, 2H), 2.21 (t, 2H), 1.5−1.1 (m, 10H), ^{31}P NMR (Varian) δ 27.6 vs 85% H_3PO_4 (s), and mass spectrometry ($M^+ = 350$).

Fabrication of Au and ITO Macroelectrodes and Interdigitated Au/ITO Microelectrode Arrays. Au macroelectrodes were made by electron beam evaporation of 50 Å Ti followed by 1000 Å Au on Si_3N_4/SiO_2 coated single crystal Si wafers. The ITO macroelectrodes were prepared by electron-beam evaporation of ITO onto Si_3N_4/SiO_2 coated Si wafers as an ITO/Au/ITO multilayer (see below). Alternatively, ITO on pre-cut glass slides was obtained from Delta Technologies (Stillwater, MN). Both the Au and ITO/Au/ITO coated wafers were subsequently cracked into 0.5 × 2.0 cm^2 pieces for electrochemical experiments.

Fabrication of the interdigitated Au/ITO microelectrode arrays generally employed techniques already detailed.[6b] Briefly, these bimetallic microelectrode arrays were prepared in a two-layer process: Si wafers were first patterned by stepping photolithography followed by electron-beam deposition of Au and lift-off, completing the Au pattern. The ITO pattern was then made by contact lithography, electron-beam deposition of an ITO(400 Å)/Au(400 Å)/ITO (400 Å) multilayer, and lift-off. This multilayer procedure produced ITO microelectrodes with good conductivity while only exposing ITO at their outside surfaces. Formation of the ITO microelectrodes in an e-beam lift-off process using only a single layer of ITO was not deemed practical because of the incompatibility of the conventional photoresist used here with the elevated substrate temperatures (200−300 °C) generally required to deposit highly-conductive, good-quality ITO films.[14] The completed bimetallic microelectrode arrays used in the thiol/carboxylic acid experiments consisted of eight individually addressable band microelectrodes, each ~2 μm wide, 0.12 μm high, 80 μm long, and with minimal separation between Au and ITO electrodes of 0.6 μm, as shown in Figure 2. The microelectrode arrays used in the thiol/phosphonic acid experiments (Figure 5) contained six individually addressable microelectrodes, three made of Au and three of the ITO/Au/ITO multilayer. These arrays were fabricated in the same fashion as just described but the electrodes were 3.7 μm wide and 220 μm long with all electrodes separated from one another by 1.3 μm.

The Au/ITO structure shown in Figure 6 was fabricated by patterning Au features on an ITO substrate, again using a conventional lift-off process. The structure in Figure 6 is therefore not a microelectrode array, since both the patterned Au and the ITO underneath are conductive. However, this patterned Au/ITO substrate was useful for imaging SIMS experiments because it was entirely conducting.

Deposition of Monolayers. Orthogonal self-assembly (OSA) of carboxylic acids and thiols was done at concentrations of 1 × 10^{-4} M in each molecule with 5% ethanol in isooctane as solvent. Techniques to maintain rigorous dryness were not used. OSA of phosphonic acids and thiols was done at concentrations of 1 × 10^{-4} to 7 × 10^{-4} M in each molecule from 30% methanol in chloroform.

The electrode cleaning procedure was as follows: sonication in acetone for 5−30 min, followed by 3−10 min exposure to a 60 W Ar plasma, and finishing with 1−5 min in a 60 W H_2 plasma generated by a Harrick plasma cleaner/sterilizer. The samples were then immediately immersed in the deposition solution.

The ITO microelectrodes were particularly sensitive to adventitious surface contamination. Great care had to be taken during the microelectrode array mounting procedure to minimize exposure to outgassing the epoxies, and cleaning times for the microelectrode arrays generally needed to be longer than those required for the macroelectrodes.

Electrochemistry. For all experiments with carboxylic acids, cyclic voltammetry was done in closed round-bottomed flasks purged with Ar using a Pine RDE4 bipotentiostat connected to a Pt gauze counter electrode and a Ag wire quasi-reference electrode. The electrolyte was recrystallized $[(n\text{-}Bu)_4]PF_6$, 0.1 M in freshly distilled acetonitrile. Prior

(11) Hickman, J. J.; Ofer, D.; Zou, C.; Wrighton, M. S.; Laibinis, P. E.; Whitesides, G. M. *J. Am. Chem. Soc.* **1991**, *113*, 1128.

(12) (a) Lee, E. J.; Banet, M.; Cook, A.; Mindas, C.; Nelson, K.; Bawendi, M.; Wrighton, M. S. In preparation. (b) Lee, E. J. Energy and Electron Transfer in Some Donor−Chromophore−Acceptor Compounds. Ph.D. Thesis, Massachusetts Institute of Technology, 1993.

(13) (a) Rabinowitz, R. *J. Org. Chem.* **1963**, *28*, 2975. (b) Degenhardt, C. R.; Burdsall, D. C. *J. Org. Chem.* **1986**, *51*, 3488. (c) See also ref 4b.

(14) Agnihotry, S.; Saini, K.; Saxena, T.; Nagpal, K.; Chandra, S. *J. Phys. D: Appl. Phys.* **1985**, *18*, 2087.

to cyclic voltammetry, and immediately upon removal from the monolayer deposition solution, all electrodes were rinsed thoroughly with hexane.

Experiments with phosphonic acids were conducted as above, but in open electrochemical cells vs SCE. The electrolyte was 0.1 M recrystallized $NaClO_4$ in 1:1 water:acetonitrile. Electrodes were rinsed with ethanol and dried under N_2 after removal from the deposition solution.

Scanning Auger Electron Spectroscopy (AES). Auger analysis was done using a Perkin-Elmer Phi 660 scanning Auger microprobe operating at beam voltages of 5−10 kV and beam currents of 3−5 nA to minimize damage to the monolayer.[1a] Samples were affixed to small pieces of copper foil with Ag paint to minimize charging.

Secondary Ion Mass Spectrometry (SIMS). SIMS images of SAMs of **II** and **V** on Au and ITO microstructures were obtained using a Fisons (VG) IX70S SIMS instrument. Details of the procedure have been previously reported.[15] The primary ion beam consisted of 27 kV Ga^+ ions. Primary ion current measured at the sample was 50 pA. Each of the images in Figure 6 was recorded over a 4.7×10^{-5} cm^2 area in 25 seconds, for a total dose to the sample of 2×10^{14} ions/cm^2 for each image.

Results and Discussion

The evidence presented here for orthogonal self-assembly takes two forms: cyclic voltammograms and high-vacuum surface spectroscopy. The combination of these techniques can provide information on the distribution and surface coverage of the molecules adsorbed to the structures of interest. Each of the molecules used in this study has a unique "tag" to make it detectable by at least one of the analytical techniques used.

Orthogonal Self-Assembly of R-COOH on ITO and R″-SH on Au. Figure 1 shows the cyclic voltammetry data for Au and ITO macromolecules derivatized in a 1×10^{-4} M solution of **I** and **III**. The coverage of both **I** and **III** on a given electrode can be determined by integrating the peaks corresponding to the acylferrocene center in **I** (+850 mV vs Ag wire) and the alkylferrocene center in **III** (+500 mV), respectively. The acyl- and alkylferrocene centers in **I** and **III** are distinguishable in each cyclic voltammogram, because their redox potentials differ by ~350 mV. Importantly, ratioing the acyl- and alkylferrocene peak areas gives a quantitative measure of the selectivities of **I** and **III** for Au and ITO. Analysis of the voltammograms in Figure 1 shows that the coverage ratio **I**:**III** is approximately 100:1 on Au and 1:45 on ITO after 30 min of immersion in the derivatizing solution. The absolute coverages of **I** on Au and **III** on ITO after 30 min are 4.4×10^{-10} and 5.8×10^{-10} mol/cm^2 which correspond to about one monolayer of each reagent on Au and ITO, respectively. Long derivatization times (15 h vs 30 min) do not detectably alter the selectivity or the coverages of the two reagents on the electrodes. In sum, the data in Figure 1 show that **I** and **III** are highly selective for Au and ITO, respectively, that each of the reagents forms a complete monolayer on its respective surface, and that this OSA process is essentially complete within 30 min.

Since the ultimate objective of this orthogonal self-assembly chemistry is to connect an array of single molecules between closely-spaced microfabricated electrodes (Scheme 2), it is important to demonstrate that the selectivity of the surface-attachment chemistry shown in Figure 1 can be reproduced on microfabricated structures. Residues left on substrates form the microfabrication process, such as photoresist, can impede or prevent attachment of molecular reagents to microfabricated electrodes. Using conventional photolithography techniques,[6b,d,e] we fabricated a partially interdigitated microelectrode array with

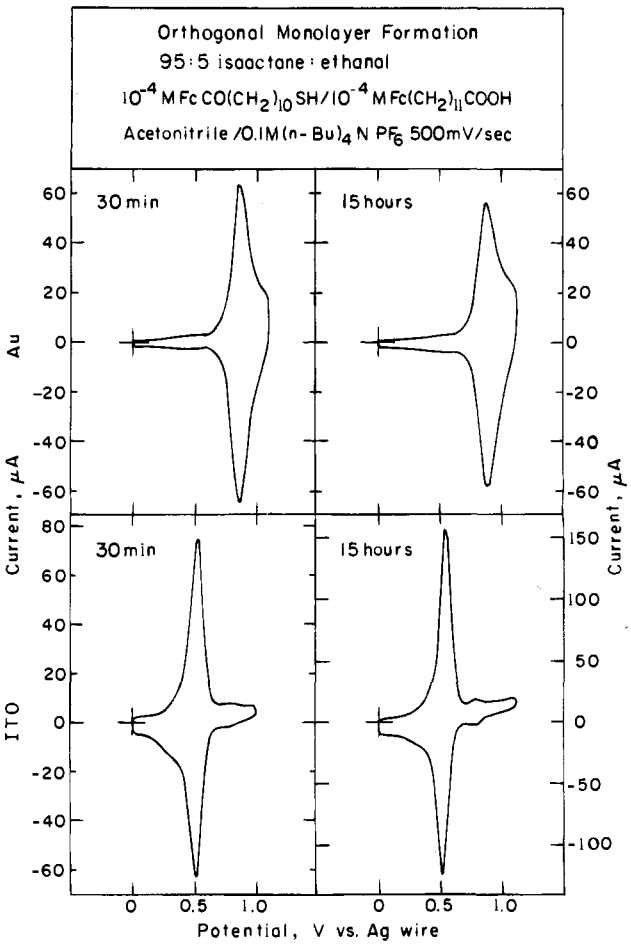

Figure 1. Cyclic voltammograns of Au and ITO macroelectrodes exposed to an equimolar solution (1×10^{-4} M) of redox-active molecules **I** and **III** for 30 min and 15 h. The coverage of **I**:**III** is approximately 100:1 on Au and 1:45 on ITO after 30 min of exposure to the derivatizing solution, as estimated by comparing the peak areas due to **I** and **III** on each electrode. Derivatization for 15 h does not change the observed selectivity. Coverage of **I** on Au: 4.4×10^{-10} mol/cm^2 (30 min and 15 h). Coverage of **III** on ITO: 5.8×10^{-10} mol/cm^2 (30 min and 15 h). Au geometrical electrode areas: 0.40 cm^2 (30 min) and 0.33 cm^2 (15 h). ITO geometrical electrode areas: 0.35 cm^2 (30 min) and 0.60 cm^2 (15 h).

4 ITO and 4 Au microelectrodes (~80 μm long × 0.1 μm thick × 2 μm wide, with Au and ITO electrodes minimally separated by 0.6 μm) on an insulating Si_3N_4 substrate, as shown in the top panel of Figure 2. OSA of thiols and carboxylic acids on the Au and ITO microwires, respectively, can be unambiguously determined by Auger electron spectroscopy and microscopy. Figure 3 shows Auger survey spectra of the Si_3N_4, ITO, and Au regions of one such Au/ITO microelectrode array exposed to a 1×10^{-4} M solution (ethanol:isooctane, 5:95) of reagents **I** and **IV**. The F peak on the ITO region marks the presence of the carboxylic acid, **IV**, on the ITO, and the absence of the F signal on the Si_3N_4 and Au surfaces demonstrates the selectivity of the carboxylic acid for ITO. No S signal from thiol **I** is present on the ITO or Si_3N_4 surfaces, consistent with the selectivity of **I** for Au. The Auger spectrum taken on Au shows a peak at 152 eV that is assigned to S,[16] confirming the presence of **I** on the Au.

More dramatic and comprehensive evidence for the selectivity of the perfluorinated carboxylic acid **IV** for the ITO microstructures is shown in the Auger element maps of the derivatized

(15) (a) Frisbie, C. D.; Martin, J. R.; Duff, R. R.; Wrighton, M. S. *J. Am. Chem. Soc.* **1992**, *114*, 7142. (b) Frisbie, C. D.; Wollman, E. W.; Martin, J. R.; Wrighton, M. S. *J. Vac. Sci. Technol. A* **1993**, *11(4)*, 2368. (c) Wollman, E. W.; Kang, D.; Frisbie, C. D.; Lorkovic, I. M.; Wrighton, M. S. *J. Am. Chem. Soc.* **1994**, *116*, 4395.

(16) A minor Au Auger peak occurs at 150 eV which cannot be easily distinguished from the S signal at 152 eV. The majority of the signal at 152 eV is due to S and not Au (see ref 11).

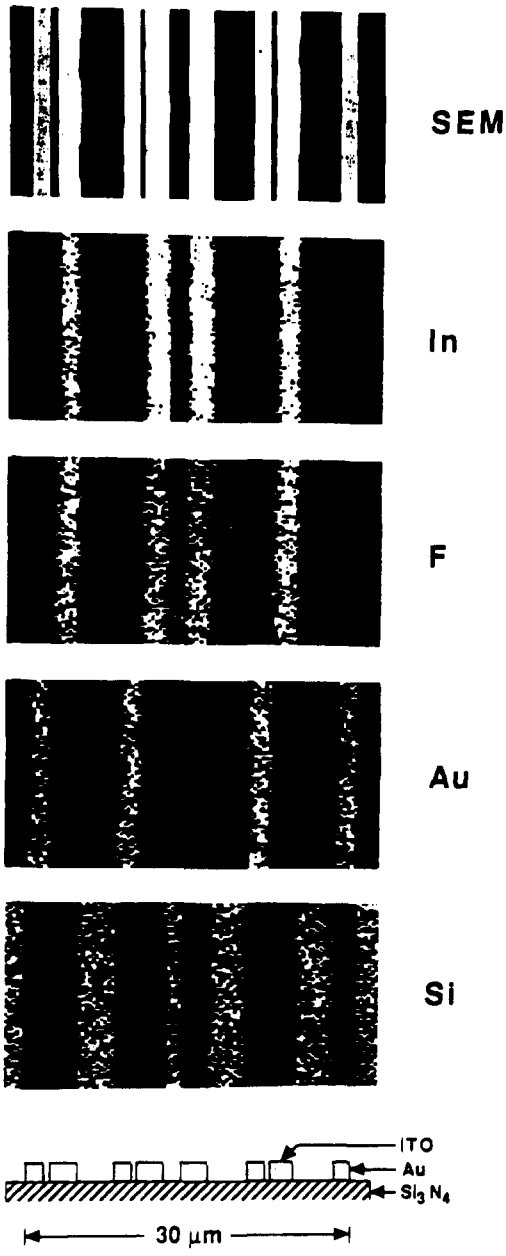

Figure 2. Au/ITO interdigitated microwires on a Si_3N_4 substrate used for demonstrating OSA. The top image is an SEM of the microstructures. Auger element maps are also included for In, F, Au, and Si from an Au/ITO interdigitated microelectrode array derivatized in an equimolar ethanol:isooctane (5:95) solution (1×10^{-4} M) of **I** and **IV**. The F signal is in registration only with the ITO microelectrodes, confirming the selective derivatization of the ITO by molecule **IV**.

Au/ITO microelectrode array included in Figure 2. The top panel of Figure 2 shows a scanning electron micrograph of the eight interdigitated Au and ITO microelectrodes. The positions of the ITO and Au electrodes are highlighted by the maps of In and Au in the second and fourth panels of the figure. The Si_3N_4 substrate is indicated by the Si map in the last panel. Importantly, an F map shown in the third panel is in registration with the ITO, and not with the Au and Si maps, demonstrating the selectivity of **IV** for the ITO microstructures. The ratio of the amount of **IV** on the ITO microwires to the amount of **IV** on the Au and Si_3N_4 surfaces is estimated to be 60:1, as determined by ratioing the average pixel intensities in the light and dark portions of the F map; essentially no difference in F counts was detected between the Au and Si_3N_4 areas of the map. For comparison, analysis of the electrochemical data on Au and ITO in Figure 1 shows nearly perfect selectivity (>100:1) of the carboxylic acid **III** for ITO. For example, after 30 min of

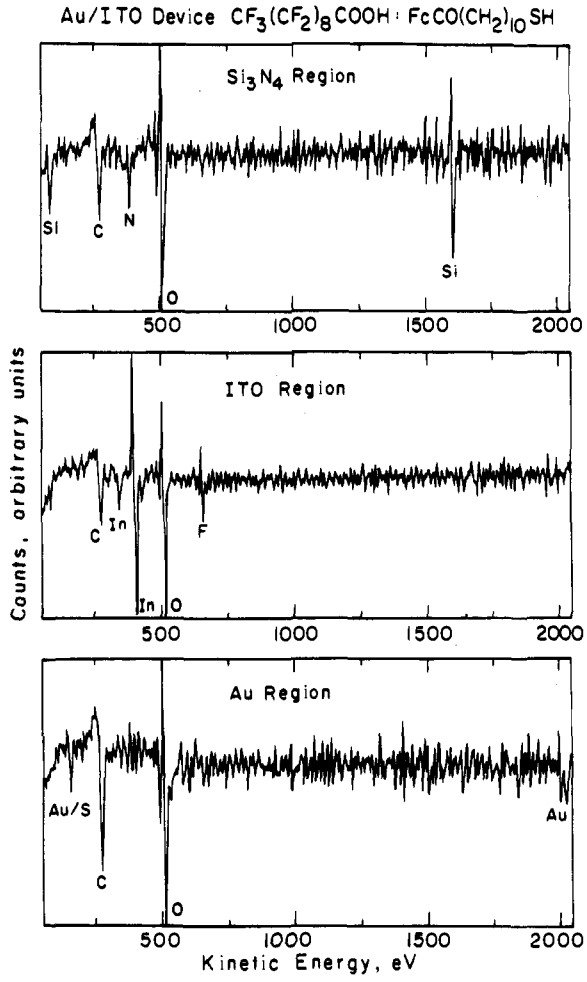

Figure 3. Auger electron spectroscopy (AES) survey scans on the Si_3N_4, ITO, and Au surfaces of an Au/ITO interdigitated microelectrode array derivatized in an equimolar ethanol:isooctane (5:95) solution (1×10^{-4} M) of thiol **I** and carboxylic acid **IV**. The signal for F arising from molecule **IV** appears on the ITO surface, and not on Au or Si_3N_4, supporting the conclusion from Figure 1 that carboxylic acids are selective for ITO. No S is detected on ITO or Si_3N_4, consistent with the selectivity of S for Au. A peak at 152 eV is shown in the Auger spectrum of Au (bottom panel) which is assigned to Au and S, indicating the presence of **I** on the Au.

derivatization, virtually no **III** is detected on Au while the coverage of **III** on ITO is 5.8×10^{-10} mol/cm^2 (see Figure 1). Thus, the detection by scanning Auger microscopy of 60 times more **IV** on ITO relative to Au in Figure 2 is qualitatively consistent with the high selectivity of carboxylic acid **III** for ITO shown in Figure 1. We have previously shown by scanning Auger microscopy that **I** assembles on Au microwires but not on the Si_3N_4 substrate.[11] Together, the data in Figures 2 and 3 clearly show that reagents **I** and **IV** attach selectively to Au and ITO microelectrodes, respectively, and not the Si_3N_4 substrate. This result, in combination with the electrochemistry shown in Figure 1, provides strong evidence that an equimolar solution of a thiol and a carboxylic acid is a viable system for OSA of a monolayer of reagents on microfabricated Au and ITO substrates, respectively. Significantly, neither derivatizing reagent binds to Si_3N_4.

Orthogonal Self-Assembly of R′-PO_3H_2 on ITO and R″-SH on Au. Investigations of self-assembled monolayers of 3-mercaptobutylphosphonic acid by Mallouk[4] suggested that phosphonic acids and thiols would also be good candidates for an OSA system. Consequently, we prepared redox-active molecule **V** to test this hypothesis. Figure 4 shows cyclic voltammograms of **I** and **V** self-adsorbed onto Au and ITO

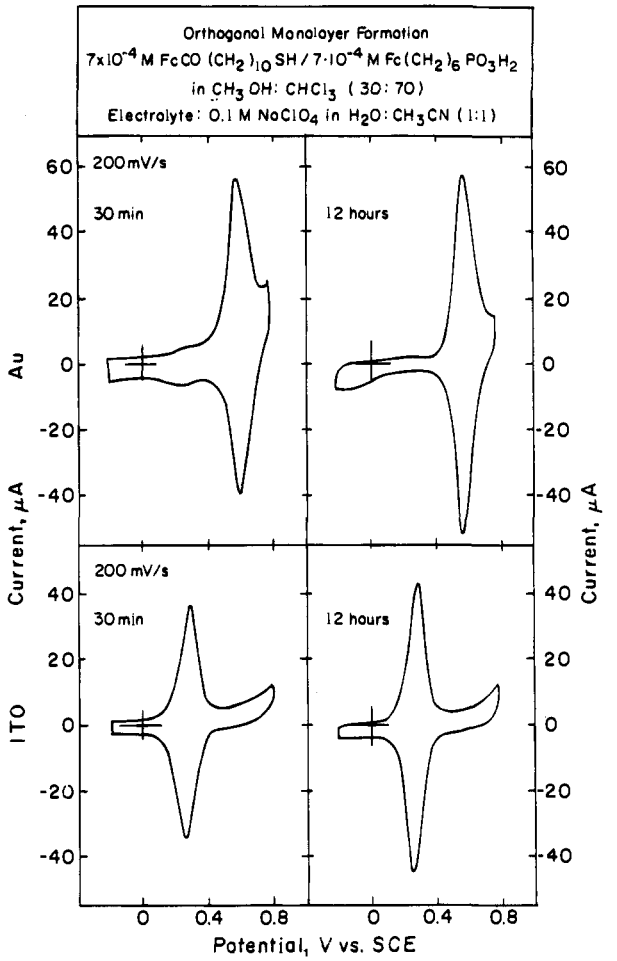

Figure 4. Cyclic voltammograms of Au and ITO macroelectrodes exposed to an equimolar (7×10^{-4} M) solution of redox-active molecules **I** and **V** for 30 min and 12 h. The coverage ratio **I**:**V** is approximately 30:1 on Au and better than 1:100 on ITO after 30 min in the derivatizing solution, as estimated by comparing the peak areas due to **I** and **V** on each electrode. Derivatization for 12 h leads to some improvement of selectivity on Au (**I**:**V** is ~100:1), with no apparent change in the selectivity on ITO. Coverage of **I** on Au: 2.6×10^{-10} mol/cm^2 (30 min) and 4.4×10^{-10} mol/cm^2 (12 h). Coverage of **V** on ITO: 2.9×10^{-10} mol/cm^2 (30 min and 12 h). Au geometrical electrode areas: 1.0 cm^2 (30 min) and 0.80 cm^2 (12 h). ITO geometrical electrode areas: 0.65 cm^2 (30 min) and 0.84 cm^2 (12 h).

macroelectrodes from a CH_3OH:$CHCl_3$ (30:70) solution with 7×10^{-4} M concentrations of each molecule. After 30 min immersion time, there is excellent selectivity of **I** for Au and **V** for ITO which improves somewhat on the Au electrode with longer immersion times (12 h). Comparison of the peak areas in the voltammograms measured at 30 min reveals a coverage ratio **I**:**V** of 30:1 on Au and better than 1:100 on ITO. The absolute coverages of **I** on Au and **V** on ITO after 30 min are 2.6×10^{-10} and 2.9×10^{-10} mol/cm^2, respectively, again corresponding to about one monolayer of redox-active molecules on each electrode. After 12 h of derivatization, the coverage of **I** on Au increases to 4.4×10^{-10} mol/cm^2 and the coverage ratio **I**:**V** on Au also increases to about 100:1. No change in coverage of reagents **I** and **V** on ITO is observed between 30 min and 12 h derivatization time; the coverage ratio remains better than 1:100 on ITO after 12 h. The data in Figure 4 thus show that **I** and **V** are strongly selective for Au and ITO, respectively, and that while there is some increase in the coverage of **I** relative to **V** on Au with longer derivatization times, good coverage and good selectivity of **I** for Au and **V** for ITO are achieved within 30 min.

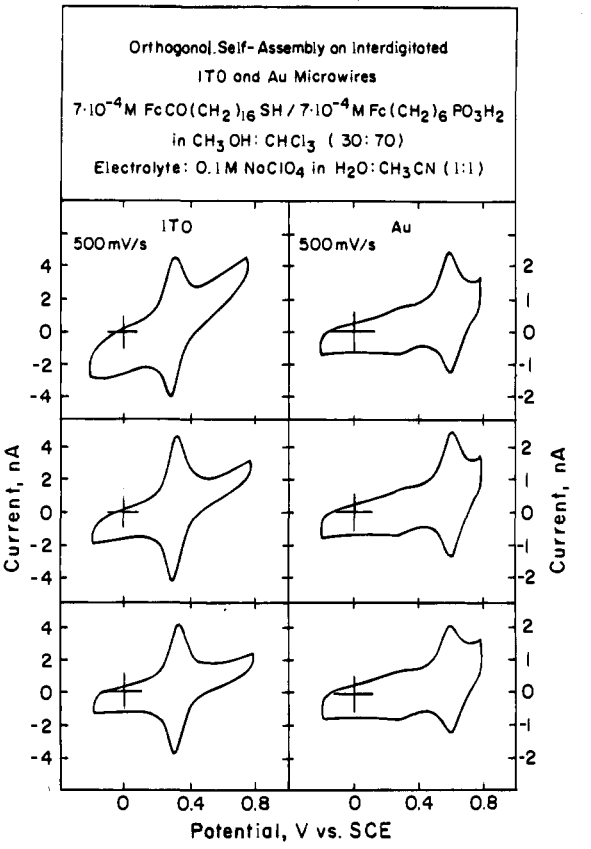

Figure 5. Cyclic voltammetry of six interdigitated Au and ITO microelectrodes derivatized for 12 h in an equimolar (7×10^{-4} M) solution of **I** and **V**. The coverage ratio of thiol to phosphonic acid (**I**:**V**) is >10:1 on the Au and better than 1:100 on the ITO. Average coverages of **I** on Au and **V** on ITO are 3.5×10^{-10} and 9.7×10^{-10} mol/cm^2, respectively. The high coverage calculated for ITO is due to the roughness of the ITO microelectrodes.[17] The geometrical area for all Au and ITO microelectrodes is 8.1×10^{-6} cm^2.

Figure 5 shows that the OSA of **I** and **V** can be reproduced on Au and ITO microstructures. We exposed an interdigitated Au/ITO microelectrode array similar (but not identical) to that shown in Figure 2 to a 7×10^{-4} M CH_3OH:$CHCl_3$ (30:70) solution of **I** and **V**. Figure 5 shows the cyclic voltammograms for each of the six interdigitated microelectrodes. No acylferrocene is detected on the ITO microelectrodes; the coverage ratio **I**:**V** is again better than 1:100. Some alkylferrocene is detected on Au, but the coverage ratio **I**:**V** is better than 10:1. Integration of the peak areas yields an average coverage of 9.7×10^{-10} mol/cm^2 of **V** on ITO[17] and 3.5×10^{-10} mol/cm^2 of **I** on Au, corresponding to roughly one monolayer of each molecule on the respective electrodes. No S, P, or Fe was detected by XPS on Si_3N_4 surfaces exposed to the same solution, indicating that neither **I** nor **V** binds to Si_3N_4.

To verify our electrochemical data demonstrating OSA of thiols and phosphonic acids on microstructures, we fabricated Au microwires on an ITO substrate, exposed this sample to a 5×10^{-4} M solution of **II** and **V**, and subsequently analyzed it by imaging SIMS. Figure 6 shows ion maps for $^{197}Au^-$, $^{19}F^-$, $^{115}In^+$, and PO_2^-, (*m*/*z* 63). The $^{19}F^-$ map is in registration with the $^{197}Au^-$ map and the PO_2^- map is in registration with $^{115}In^+$, confirming the selectivity of the F-containing thiol **II** for Au and phosphonic acid **V** for ITO. A more quantitative

(17) The high coverage on the ITO is due to the roughness of the ITO/Au/ITO multilayer electrodes. This roughness is an artifact of our e-beam deposition and lift-off procedure, which can result in microelectrodes with "burrs" which increase the total surface area of the electrodes. In the case of this bimetallic microelectrode array, the burrs could not be removed from the ITO structure despite vigorous sonication in CH_3OH.

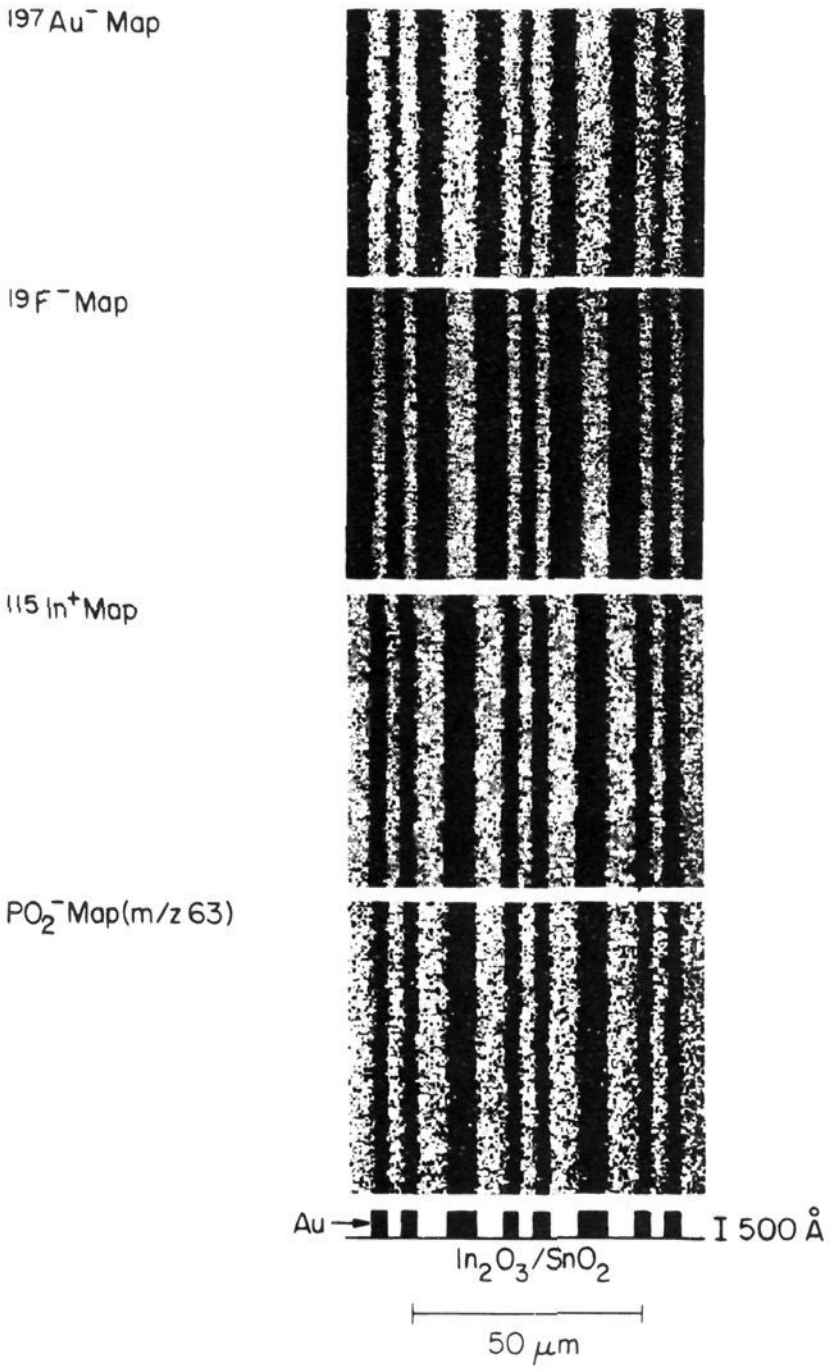

Figure 6. SIMS maps of $^{197}Au^-$, $^{19}F^-$, $^{115}In^+$, and PO_2^- (m/z 63) ions of a Au/ITO microstructure exposed to an equimolar (5×10^{-4} M) methanol:chloroform (30:70) solution of **II** and **V** for 12 h. The $^{19}F^-$ signal is in registration with the Au, and the PO_2^- is in registration with the ITO, demonstrating the orthogonal self-assembly of the molecules. Each image represents a 75×62 μm^2 area and was acquired in 25 s using a 50 pA, 27 keV Ga^+ primary ion beam.

analysis of the images shows that the ratio of the coverage of **II** on Au to the coverage of **II** on ITO is ~50:1, as determined by ratioing the average pixel intensities in the light and dark regions of the F map. The ratio of **V** on ITO to **V** on Au can be determined from the PO_2^- map in a similar fashion and is ~15:1. Referring to Figure 5, it can be estimated that the selectivity of **I** for Au microwires relative to ITO microwires is at least 100:1 since no coverage of **I** is detected on the ITO. Also from Figure 5, the selectivity of **V** for ITO microwires is at least 10:1, as determined by comparing the coverages of **V** on the ITO and Au microwires. The high selectivity of reagents **II** and **V** for Au and ITO observed in the SIMS maps in Figure 6 is thus qualitatively consistent with the electrochemical data for OSA of reagents **I** and **V** on Au and ITO microwires shown in Figure 5. From the data in Figures 4–6 we conclude that thiols and phosphonic acids present in the same solution at equimolar concentration self-assemble orthogonally on Au and ITO microstructures in a manner analogous to that of thiols and carboxylic acids.

Comparison of R-COOH and R′-PO_3H_2 for OSA in the Presence of R″-SH. In general, we have found that phosphonic acids bind to ITO more aggresively than carboxylic acids, based on the observed coverage ratios **I**:**III** and **I**:**V** on ITO. Specifically, comparison of the data in Figures 1 and 4 shows that no thiol adsorbs to ITO when phosphonic acid is present in the same solution (Figure 4), while there is some persistent adsorption of thiol to ITO in the presence of carboxylic acid (Figure 1). We have found that immersion of ITO in solutions containing only **I** results in persistent low coverage ($\sim 3 \times 10^{-11}$ mol/cm^2) of **I** on the ITO. Self-adsorption of a redox-active thiol on ITO has also been reported by others, but the mechanism for adsorption is unclear.[18] Thus, it appears that competition of carboxylic or phosphonic acids with thiols for ITO binding sites is necessary to achieve highly selective coverage of either acid on the ITO. Comparison of the data in Figures 1 and 4 indicates that, relative to thiols present in the same solution, phosphonic acids compete for binding sites on ITO better than carboxylic acids, since no thiol is detected on ITO electrodes exposed to equimolar solutions of thiol and phosphonic acid.

Factors which could affect the overall surface selectivities of either carboxylic acids, phosphonic acids, or thiols for Au and ITO include hydrocarbon chain length in the molecules and the specific solvent used for monolayer deposition. These factors are currently under investigation. Our preliminary studies have shown that there is a solvent dependence on the surface selectivities for the thiol/carboxylic acid system. Specifically, we found that a two-component solvent mixture consisting of 5% ethanol in isooctane proved to be the most successful for OSA of **I** and **III**, providing rapid monolayer formation, good surface coverage, and high selectivity, as evidenced in Figure 1. Less selectivity of **I** for Au, that is, greater coverage of **I** on ITO, was observed for higher ratios of ethanol:isooctane and for all ethanol:hexane solutions of the two molecules. This observation can be explained qualitatively by noting that molecule **III** is less soluble in the ethanol:isooctane (5:95) solvent mixture than in solvents with higher ratios of ethanol:isooctane and in all ethanol:hexane solvents. Lower solubility presumably makes **III** chemisorb more aggressively on the ITO, so that **III** competes more effectively with **I** for ITO binding sites in the ethanol:isooctane (5:95) solvent system. Variations in the solvent composition can thus be used to tune the OSA process to produce the maximum surface selectivity of the surface-attachment ligands.

Conclusions

Orthogonal self-assembly has been achieved for Au and ITO substrates simultaneously exposed for 30 min to an equimolar solution of (1) a thiol and a carboxylic acid or (2) a thiol and a phosphonic acid. Verification that OSA occurred was provided by a combination of techniques, including cyclic voltammetry of redox-tagged molecules **I**, **III**, and **V** and AES, XPS, and SIMS surface chemical characterizations. Importantly, OSA has been demonstrated for several pairs of microfabricated, interdigitated Au and ITO electrodes, where the minimal spacing between the two electrodes is <1 μm; neither derivatizing reagent binds to the Si_3N_4 substrate. Present nanofabrication technology can be used to place two electrodes <50 nm apart.[19] Nanofabrication in combination with OSA is therefore a promising method for orienting and connecting individual macromolecules between externally addressable contacts.

Acknowledgment. This research was supported by the National Science Foundation. M.S.W. thanks Professor T. E. Mallouk for suggesting the use of phosphonates to form monolayers on ITO. The authors also thank Dr. E. W. Wollman for the synthesis of 12-ferrocenyldodecanoic acid.

JA943637P

(18) Obeng, Y. S.; Bard, A. J. *Langmuir* **1991**, *7*, 195.
(19) (a) Chu, W.; Smith, H. I.; Schattenburg, M. L. *Appl. Phys. Lett.* **1991**, *59*, 1641. (b) Wang, Y.; Chou, S. Y. *J. Vac. Sci. Technol. B* **1992**, *10*, 2962.